JACS
JOURNAL OF THE AMERICAN CHEMICAL SOCIETY

COMMUNICATION

pubs.acs.org/JACS

Single Particle Orientation and Rotation Tracking Discloses Distinctive Rotational Dynamics of Drug Delivery Vectors on Live Cell Membranes

Yan Gu, Wei Sun, Gufeng Wang, and Ning Fang*

Ames Laboratory, U.S. Department of Energy and Department of Chemistry, Iowa State University, Ames, Iowa 50011, United States

Supporting Information

ABSTRACT: Engineered nanoparticles have emerged as potentially revolutionary drug and gene delivery vectors. Using rod-shaped gold nanoparticles as a model, we studied for the first time the rotational dynamics of nanoparticle vectors on live cell membranes and its impact on the fate of these nanoparticle vectors. The rotational motions of gold nanorods with various surface modifiers were tracked continuously at 200 frames/s under a differential interference contrast microscope. We found that the rotational behaviors of gold nanorod vectors are strongly related to their surface charges. Specific surface functional groups and the availability of receptors on cell membranes also contribute to the rotational dynamics. The study of rotational Brownian motion of nanoparticles on cell membranes will lead to a better understanding of the mechanisms of drug delivery and provide guidance in designing surface modification strategies for drug delivery vectors under various circumstances.

Among the numerous drug delivery strategies that have been developed to overcome the physiological barrier of the cell and nuclear membranes,[1] engineered nanoparticles have emerged as potentially revolutionary drug carriers for diagnosis and treatment of many diseases[2] because of their advantages including enhanced drug solubility, improved internalization efficiency, targeted delivery to the diseased organ, controlled drug release, and reduced side effects. For example, gold nanoparticles have been used to deliver drugs[3−5] and biological molecules.[6−10]

In order to rationally design nanoparticle carriers, it is imperative to understand the influences of the nanoparticles' physical and chemical properties, including particle size, shape, and surface characteristics, on nanoparticle-based drug delivery.[2,11] Most of the reported research efforts in this area have been focused on identifying these effects from static fluorescence and electron micrographs taken at different stages;[12−17] however, the characteristic translational and rotational dynamics of functionalized nanoparticle carriers resulting from their interactions with the cellular environment has not been fully elucidated.

Conventional single particle tracking (SPT)[18] techniques are useful for probing the structure and biological functions of cell membranes at the molecular level, but their usefulness is limited to the study of translational motions. To overcome this limitation, plasmonic gold nanorods with anisotropic absorption and scattering properties have been utilized as orientation probes under dark-field microscopy,[19,20] photothermal imaging,[21] and Nomarski-type differential interference contrast (DIC) microscopy.[22] These methods have been successfully employed in characterizing well-defined rotational motions such as the rotational motion of the center domain of F1-ATPase immobilized on a glass substrate[20] by resolution of the nanorod orientation in each image frame of a recorded rotation sequence. On the other hand, the characterization of the rotational Brownian motion requires statistical analysis on a large number of consecutive images taken at high frame rates. Pierrat et al.[23] demonstrated that the two-dimensional rotational dynamics of laterally frozen nanoparticles on synthetic membranes is controlled in part by dragging forces introduced by the surface viscosity of the membrane; however, the rotational Brownian motion of functionalized nanoparticles on live cell membranes has never been elucidated.

In the present study, the integrated imaging platform based on DIC microscopy for single particle orientation and rotation tracking (SPORT)[22] was employed for direct visualization of the distinctive rotational dynamics of gold nanorods functionalized with different surface modifiers on live cell membranes. Images of both the cell and the nanoparticle vectors were acquired at 200 frames per second (fps) under a DIC microscope, which provides a unique advantage of visualizing fast rotational and translational motions of nanoparticle probes and the cellular environment simultaneously with sufficient angular resolution.[22,24,25]

Gold nanorods with an average size of 25 nm × 73 nm were surface-modified with polyethylene glycol (PEG), carboxyl-terminated PEG (PEG−CO_2^{2-}), transferrin[26] through PEG linkers, trans-activating transcriptional (TAT) activator (a cell-penetrating peptide from human immunodeficiency virus 1[17,27,28]) through PEG linkers, and two forms of polyether imide (PEI): linear 22 kDa and branched 25 kDa (see Supplementary Figure 1 in the Supporting Information for illustrations of the functionalized nanorods). All of these modifiers except PEG−CO_2^{2-} have been used as either gene/drug delivery agents or agents that promote the delivery efficiencies of nanoparticle carriers.

The functionalized gold nanorods were tracked continuously to reveal their rotational dynamics until they were internalized by the cells or stayed on the membrane sufficiently long (>2 h) in noninternalization cases. Movie 1 in the Supporting Information shows an example in which a PEG−CO_2^{2-}-modified gold nanorod exhibited both translational and rotational motions on

Received: January 20, 2011
Published: March 25, 2011

dx.doi.org/10.1021/ja200603x | J. Am. Chem. Soc. 2011, 133, 5720–5723

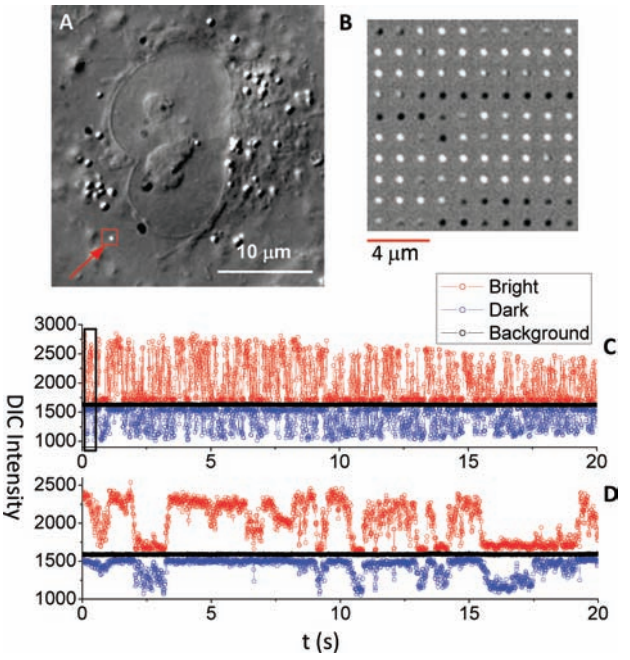

Figure 1. (A) DIC image of an A549 cell with a PEG−CO_2^{2-}-modified gold nanorod highlighted in the red square. (B) Composite of 100 consecutive images of the gold nanorod. (C, D) Typical DIC intensity traces as functions of time for (C) fast and (D) slow rotations. The rectangle in (C) distinguishes the intensities of the 100 DIC images shown in (B). The fast-rotation trace was recorded right after the nanorod landed on the cell membrane, and the slow-rotation trace was recorded 7 min later for the same nanorod.

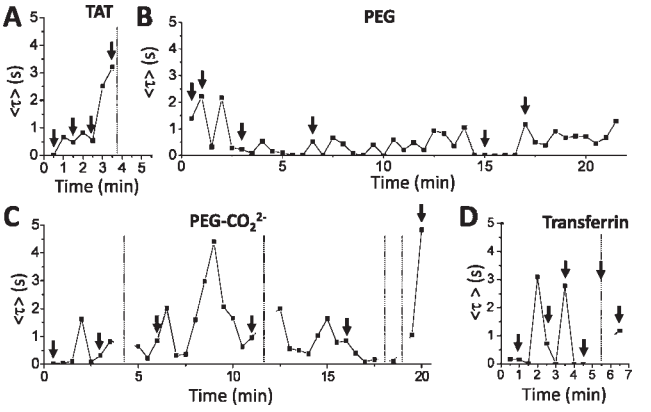

Figure 2. Representative evolutions (at a time interval of 0.5 min) of the mean relaxation times $\langle\tau\rangle$ of (A) TAT-, (B) PEG-, (C) PEG−CO_2^{2-}-, and (D) transferrin-modified gold nanorods on live cell membranes. Each data point was calculated from 4000 frames in a 20 s movie. The dotted vertical lines indicate the pauses of rotation, for which no mean relaxation times were calculated. The arrows point out the movie segments that are included in the corresponding movies in the Supporting Information.

the membrane of an A549 human lung cancer cell. Unlike spherical probes, the gold nanorods displayed flickering bright/dark images for active rotational motions under the DIC microscope. Figure 1 shows the DIC intensities of the gold nanorod in 4000 consecutive images acquired at 200 fps. The two DIC intensity traces present typical fast (Figure 1C) and slow (Figure 1D) rotations of the gold nanorod as revealed by the frequencies of the DIC intensity variations of both the bright and dark parts.

To semiquantify the rotational dynamics of gold nanorods, we analyzed the stochastic DIC intensity fluctuations using the autocorrelation function.[29−31] The DIC contrast, which is defined as the difference between the bright intensity and the dark intensity divided by the background intensity, was used as the signal in computing an autocorrelation function for 4000 consecutive images in each movie. The autocorrelation curve could be satisfactorily fitted with a stretched exponential function[29−31] (see the Supporting Information for details). The mean relaxation time $\langle\tau\rangle$ for the decay of the autocorrelation function reflects the rotational speed of the gold nanorod, with a smaller $\langle\tau\rangle$ value corresponding to faster rotation. Mean relaxation times of 0.02 s for the fast rotation in Figure 1C and 0.48 s for the slow rotation in Figure 1D were obtained through nonlinear least-squares fitting (Supplementary Figure 2).

Using the autocorrelation analysis, we found that the time evolution of the rotational dynamics of gold nanorods was tightly related to their surface charges. The functionalized nanoprobes can be categorized according to their surface charges: positively charged (TAT, linear or branched PEI), neutral (PEG), and negatively charged (PEG−CO_2^{2-}, transferrin). The positively charged particles were adsorbed quickly by the negatively charged cell membrane through electrostatic interactions, while the neutral or negatively charged particles were captured at much lower rates and usually had much longer durations of active rotation on the cell membrane. For each type of functionalized nanoparticle vector, multiple examples were recorded, and all of them demonstrated similar characteristic rotational dynamics.

We begin our detailed discussion with the simplest case: the linear or branched PEI-modified gold nanorods. These nanorods were strongly positively charged, and they lost their rotation almost immediately after appearing on the cell membrane because of strong electrostatic interactions. In Movie 2, a nanorod modified with branched 25 kDa PEI showed little rotation for the entire 20 s recording time. Some slight changes in the DIC intensity were likely caused by the fluidity of the membranes.

TAT peptide is among the most widely used cell-penetrating reagents. Although the mechanism by which TAT peptide enters cell membranes is still under debate, it is generally believed that a multiplicity of pathways are involved in the internalization process.[32] The TAT-modified gold nanorods with a ζ potential of +22.3 mV had much weaker positive charges than the PEI-modified nanorods, resulting in longer periods of active rotation on the membrane. Movie 3 presents six movie segments, displayed side-by-side, showing the same TAT-modified nanorod at different times after its appearance on the cell membrane. The corresponding DIC intensity traces are displayed in Supplementary Figure 3. The mean relaxation time increased gradually within the first 4 min (Figure 2A), most likely because the TAT peptides on the nanorod surface were incorporated more and more effectively into the membrane. The nanorod rotation became very slow and nearly came to a stop after ~4 min on the membrane. This nanorod was eventually internalized by the cell. Similar observations were recorded for other TAT-modified gold nanorods.

PEG is a neutral polymer that is well-known for resisting nonspecific adsorption.[33] The PEG-modified gold nanorods (ζ = +1.5 mV) showed evident reluctance to bind firmly to the cell

dx.doi.org/10.1021/ja200603x | J. Am. Chem. Soc. 2011, 133, 5720–5723

membrane. Desorption of the PEG-modified nanorods from the membrane occurred frequently. During the whole time these nanorods were adsorbed onto the membrane, they showed active lateral movement while maintaining a high speed of rotation (Figure 2B, Movie 4, and Supplementary Figure 4). No internalization events were observed before the cells lost their viability on the microscope stage.

The PEG$-CO_2^{2-}$-modified gold nanorods had negative surface charges ($\zeta = -20$ mV); thus, it was difficult for them to be adsorbed onto the negatively charged cell membrane because of electrostatic repulsion. When they did land on the membrane through nonspecific binding to the cationic sites, many of them desorbed from the membrane within seconds to minutes, similar to the PEG-modified nanorods. For those nanorods that stayed on the membrane, the fluctuation in rotation speed was much more significant than that for the PEG-modified nanorods. Their rotation could slow down significantly or even come to full stop for up to a few minutes and then become fast again, showing the struggles between the weak binding interactions and thermal activity of the nanorod and its surrounding environment. Figure 2C, Movie 5, and Supplementary Figure 5 show an example in which a nanorod rotated for a prolonged period (with the rotation stopping occasionally) before finally becoming anchored on the membrane.

Finally, transferrin is a naturally occurring plasma protein involved in iron delivery. The internalization of transferrin involves specific binding to the transferrin receptors on the cell membrane.[34] Similar to the PEG$-CO_2^{2-}$-modified gold nanorods, the transferrin-modified nanorods ($\zeta = -11.2$ mV) also showed reluctance to bind onto the cell membrane because of the negative charges on their surfaces. However, once they were bound to the cell surface, their active rotation lasted much less time than that of the PEG$-CO_2^{2-}$-modified ones. Figure 2D, Movie 6, and Supplementary Figure 6 show such an event, during which the transferrin-modified nanorod was endocytosed within 7 min after it was adsorbed onto the membrane. While the nanorod stayed at the initial landing site on the membrane, its rotation was initially fast, slowed down significantly, and then quickly became fast again. This pattern of speed change happened twice before the nanorod moved laterally to a new site. At this new location, the nanorod stopped rotating for ~25 s and then was endocytosed by the cell. The lateral movement likely involved a change of binding from a nonspecific site to transferrin receptors, thus facilitating receptor-mediated endocytosis. As a comparison, it usually took a much longer time (tens of minutes to hours) for the PEG$-CO_2^{2-}$-modified gold nanorods to be anchored on the cell membrane because of the lack of specific receptors. Thus, for the first time, the distinctive rotational behaviors of the transferrin- and PEG-CO_2^{2-}-modified nanorods have been revealed and convincingly attributed to the availability of specific binding sites on the cell membrane.

In summary, we have studied the real-time rotational dynamics of variously functionalized gold nanoparticle vectors on live cell membranes for the first time. The rotational behaviors of the gold nanorods were strongly related to the surface charges. Specific surface functional groups and the availability of receptors on the cell membrane also contribute to the rotational dynamics of the gold nanorods. Because the gold nanorods were nonblinking and nonbleaching, they could be tracked continuously for a much longer time than in the case of fluorophore-based techniques. The study of rotational behaviors of gold nanoparticles on live cells can be extended to other cellular processes, such as endocytosis, exocytosis, intracellular transport, and cell−cell communication, thus bringing us further on the exploration into the cell kingdom. More significantly, studies of the rotational Brownian motion of nanoparticles on cell membranes will lead to a better understanding of nanoparticle-based drug delivery mechanisms and provide guidance in designing modification strategies for drug delivery vectors under various circumstances.

■ ASSOCIATED CONTENT

Supporting Information. Materials and methods, supplementary figures, and Quicktime movies. This material is available free of charge via the Internet at http://pubs.acs.org.

■ AUTHOR INFORMATION

Corresponding Author
nfang@iastate.edu.

■ ACKNOWLEDGMENT

This work was supported by U.S. Department of Energy, Office of Basic Energy Sciences, Division of Chemical Sciences, Geosciences, and Biosciences. The Ames Laboratory is operated for the U.S. Department of Energy by Iowa State University under Contract DE-AC02-07CH11358.

■ REFERENCES

(1) Dass, C. R.; Choong, P. F. M. *Peptides* **2006**, *27*, 3020.
(2) Petros, R. A.; DeSimone, J. M. *Nat. Rev. Drug Discovery* **2010**, *9*, 615.
(3) Cheng, Y.; Samia, A. C.; Li, J.; Kenney, M. E.; Resnick, A.; Burda, C. *Langmuir* **2010**, *26*, 2248.
(4) Dreaden, E. C.; Mwakwari, S. C.; Sodji, Q. H.; Oyelere, A. K.; El-Sayed, M. A. *Bioconjugate Chem.* **2009**, *20*, 2247.
(5) Patra, C. R.; Bhattacharya, R.; Mukherjee, P. *J. Mater. Chem.* **2009**, *20*, 547.
(6) Giljohann, D. A.; Seferos, D. S.; Prigodich, A. E.; Patel, P. C.; Mirkin, C. A. *J. Am. Chem. Soc.* **2009**, *131*, 2072.
(7) Kawano, T.; Yamagata, M.; Takahashi, H.; Niidome, Y.; Yamada, S.; Katayama, Y.; Niidome, T. *J. Controlled Release* **2006**, *111*, 382.
(8) Lee, J.-S.; Green, J. J.; Love, K. T.; Sunshine, J.; Langer, R.; Anderson, D. G. *Nano Lett.* **2009**, *9*, 2402.
(9) Wijaya, A.; Schaffer, S. B.; Pallares, I. G.; Hamad-Schifferli, K. *ACS Nano* **2009**, *3*, 80.
(10) Zheng, B.; Yamashita, I.; Uenuma, M.; Iwahori, K.; Kobayashi, M.; Uraoka, Y. *Nanotechnology* **2010**, *21*, No. 045305.
(11) Verma, A.; Stellacci, F. *Small* **2010**, *6*, 12.
(12) Chithrani, B. D.; Chan, W. C. W. *Nano Lett.* **2007**, *7*, 1542.
(13) Chithrani, B. D.; Ghazani, A. A.; Chan, W. C. W. *Nano Lett.* **2006**, *6*, 662.
(14) Cho, E. C.; Xie, J. W.; Wurm, P. A.; Xia, Y. N. *Nano Lett.* **2009**, *9*, 1080.
(15) Huang, H.-C.; Barua, S.; Kay, D. B.; Rege, K. *ACS Nano* **2009**, *3*, 2941.
(16) Callahan, J.; Kopeček, J. *Biomacromolecules* **2006**, *7*, 2347.
(17) Tkachenko, A. G.; Xie, H.; Liu, Y. L.; Coleman, D.; Ryan, J.; Glomm, W. R.; Shipton, M. K.; Franzen, S.; Feldheim, D. L. *Bioconjugate Chem.* **2004**, *15*, 482.
(18) Saxton, M. J. *Nat. Methods* **2008**, *5*, 671.
(19) Sonnichsen, C.; Alivisatos, A. P. *Nano Lett.* **2005**, *5*, 301.
(20) Spetzler, D.; York, J.; Daniel, D.; Fromme, R.; Lowry, D.; Frasch, W. *Biochemistry* **2006**, *45*, 3117.
(21) Chang, W. S.; Ha, J. W.; Slaughter, L. S.; Link, S. *Proc. Natl. Acad. Sci. U.S.A.* **2010**, *107*, 2781.

(22) Wang, G. F.; Sun, W.; Luo, Y.; Fang, N. *J. Am. Chem. Soc.* **2010**, *132*, 16417.
(23) Pierrat, S.; Hartinger, E.; Faiss, S.; Janshoff, A.; Sonnichsen, C. *J. Phys. Chem. C* **2009**, *113*, 11179.
(24) Pluta, M. *Advanced Light Microscopy*; Elsevier Science Publishing: New York, 1989; Vol. 2.
(25) Sun, W.; Wang, G.; Fang, N.; Yeung, E. S. *Anal. Chem.* **2009**, *81*, 9203.
(26) Qian, Z. M.; Li, H. Y.; Sun, H. Z.; Ho, K. *Pharmacol. Rev.* **2002**, *54*, 561.
(27) de la Fuente, J. M.; Berry, C. C. *Bioconjugate Chem.* **2005**, *16*, 1176.
(28) Heitz, F.; Morris, M. C.; Divita, G. *Br. J. Pharmacol.* **2009**, *157*, 195.
(29) Hess, S. T.; Webb, W. W. *Biophys. J.* **2002**, *83*, 2300.
(30) Martin, J. E.; Wilcoxon, J.; Odinek, J. *Phys. Rev. A* **1991**, *43*, 858.
(31) Rocker, C.; Potzl, M.; Zhang, F.; Parak, W. J.; Nienhaus, G. U. *Nat. Nanotechnol.* **2009**, *4*, 577.
(32) Brooks, H.; Lebleu, B.; Vives, E. *Adv. Drug Delivery Rev.* **2005**, *57*, 559.
(33) Xie, J.; Xu, C.; Kohler, N.; Hou, Y.; Sun, S. *Adv. Mater.* **2007**, *19*, 3163.
(34) Li, H.; Qian, Z. M. *Med. Res. Rev.* **2002**, *22*, 225.